Kasetsart J. (Nat. Sci.) 48 : 815 - 822 (2014)

Electrical Properties of Bi-Layered Nanostructured Au/Indium Tin Oxide Thin Films

Tula Jutarosaga[1,2,*], Prayoon Suapadkron[1,2], Rungroj Tuayjareon[1,2], Chumphon Luangchaisri[1] and Supattanapong Dumrongrattana[1,2]

ABSTRACT

Au thin films were deposited on 150-nm thick indium tin oxide (ITO)/glass using a simple direct current sputtering technique. The Au thickness was varied from approximately 8 nm to 34 nm. As-deposited bi-layered Au/ITO thin films were then characterized using a four-point probe technique and Hall measurement to identify their electrical properties. The results showed that there was a substantial contribution from the Au films on the electrical conductivity of the bi-layered material, even when a discontinuous Au nanostructure was observed on the ITO films. A simple circuit model was developed to identify the electrical behavior of this bi-layered material. The increase in the carrier concentration and the reduction in carrier mobility was possibly a result of the interfaces between the Au islands and the ITO film.

Keywords: electrical resistivity, metallic thin films, bi-layered thin films, four-point probe

INTRODUCTION

Indium tin oxide (ITO) film, one among many metal oxide films, has been extensively used as transparent conducting film, for example in flat-panel displays (Klinghult and Futter, 2009), and photovoltaic applications (Feng and Ghosh, 1979). The important characteristics of ITO are transparency and high conductivity, though the number of studies on this type of material is increasing (Pokaipisit *et al.*, 2007; Aiempanakit *et al.* 2008), with the new discovery of high-conductive graphene (Novoselov *et al*., 2004). In previous studies, various structures of transparent conductive films were fabricated (Bender *et al.*, 1998; Ke *et al.*, 2005; Choi *et al.*, 2009). To improve the electrical conductivity of the metal oxide thin film, metal/metal oxide or metal oxide/metal/metal oxide thin films such as Au/ITO (Ke *et al.*, 2005), ITO/AgCu/ITO (Bender *et al.*, 1998) or ITO/Pt/ITO (Choi *et al.*, 2009) were fabricated and investigated. An example of the usage of Au/ITO films was to improve the efficiency of a polymer light-emitting device where the Au layers provided the suitable energy level alignment to enhance hole injection (Ke *et al.*, 2005). In addition, ITO-metal-ITO (IMI) structures show higher conductivity than the pure ITO thin films; while the transparency to visible light is still acceptable at above 80% (Bender *et al.*, 1998).

[1] Department of Physics, Faculty of Science, King Mongkut's University of Technology Thonburi, Bangkok 10140, Thailand.

[2] Thin Film Technology Research Laboratory, ThEP Center, CHE, 328 Si Ayutthaya Rd., Ratchathewi, Bangkok 10400, Thailand.

* Corresponding author, e-mail: tula.jut@mail.kmutt.ac.th

Received date : 15/10/13 Accepted date : 09/07/14

In the current study, the sheet resistance was investigated of simple bi-layered Au/ITO thin films on borosilicate glass substrate with various Au thicknesses from an island-like structure to a continuous thin film. Vu *et al.*, (1991) reported the bi-layered sheet resistance was a function of the sheet resistance of each layer with the specific contact resistance described by a simple transmission line model. A stage of incomplete coating of thin films has been rarely explored, especially as island-like, bi-layered thin films. Understanding the electrical properties of the early stage of the film's growth through the resistance may provide a better idea of the physics of the interface. Therefore, the resistance of the simple sputter-deposited Au nanoparticles on ITO/glass substrate with various sputtering times was investigated using a simple four-point probe technique.

A four-point probe is one of many common methods for measuring the sheet resistance of a semiconductor material and consists of two probes supplying the current and two probes measuring the voltage (Schroder, 1998). The technique has been modified for other purposes; for example, the four-point-probe-field-effect technique was used for the measurement of the electrical characteristics of thin films for field effect transistors to characterize these bi-layered thin films (Nakamura *et al.*, 2003). As shown in Figure 1, the current flows in and out of the material between two outside probes (probes 1 and 4), while the voltages are measured by other two probes (probes 2 and 3). This schematic diagram shows the contact resistance (R_c), effected from the metal probe contact with the material, and the current spreading resistance (R_{sp}), arise from the current when it flows into or out of the material.

These resistances are negligible because the voltage is measured by a high- impedance voltmeter. The sheet resistance (R_{sheet}) can be calculated by $R_{sheet} = F(V/I)$ where V is a voltage form voltmeter, I is the current supplied between two probes and F is a correction factor. The correction factor is described as a product of three separate correction factors: $F = F_1 \times F_2 \times F_3$ where F_1 is a correction factor for material thickness, F_2 is a correction factor for lateral dimensions and F_3 is a correction factor for placement of probes. For very thin specimens, the sheet resistance R_{sheet} can be calculated from Equation 1 (Schroder, 1998):

$$R_{sheet} = \frac{\pi}{\ln(2)}\left(\frac{V}{I}\right) \quad (1)$$

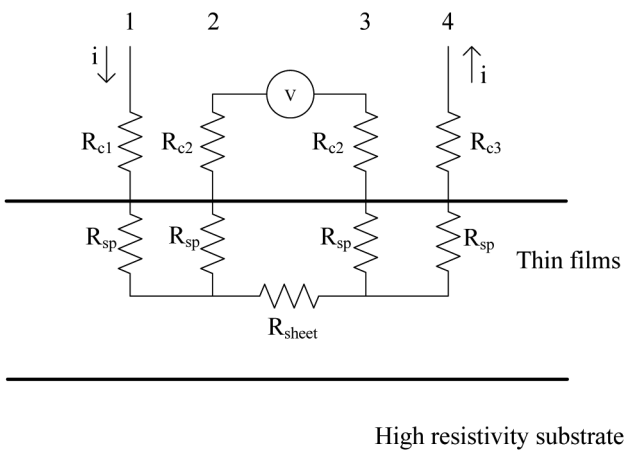

Figure 1 Schematic diagram of four-point probe measurement (R_c = Contact resistance; R_{sp} = Current spreading resistance; R_{sheet} = Sheet resistance; v = Voltage between probe 2 and probe 3; i = Current between probe 1 and probe 4; numbers indicate probes).

where V is the voltage measured in volts and I is the current between two probes measured in amperes.

The current experiment employed a four-point probe to investigate the influence of Au nanoparticles on the electrical resistance of bi-layered Au/ITO films as there have been few reports on the circuit model explaining the effect of the discontinuous Au clusters on the overall electrical properties of the bi-layered thin films. For the simplicity of the analysis, the resistance was used instead of sheet resistance. According to Equation 1, the resistance and sheet resistance can be interchanged using the factor of π / ln(2) as the resistance is equal to V / I. Based on the parallel circuit model (Barborini *et al.*, 2010), the total resistance could simply be calculated from the resistance of Au and ITO.

MATERIAL AND METHODS

The Au thin films were deposited on commercially available 150-nm thick ITO/glass and microscopic glass substrates using a simple, direct current, sputtering method. The schematic diagram of fabricated films is shown in Figure 2. The Polaron SC7620 sputter coater (Quorum Technologies Ltd, Ashford, UK) with the 57mm-diameter Au target was used for coating Au layers on: 1) ITO/glass substrates and 2) bare glass substrates. The experimental conditions are shown in Table 1, with the coating times varied in a non-rotation sample holder.

The coating time was stepped up from 4 to 17 min in 1 min increments. The film resistances were measured using the four-point probe (Signatone Pro4 S-302-4; Lucas Signatone Corp., Gilroy, CA, USA). The current source was a high-voltage-source meter (Keithley 2410; Keithley Instruments, Inc., Cleveland, OH, USA). The mobility and carrier concentration were measured using the Hall Effect measurement by the van der Pauw method (Schroder, 1998) at room temperature (electric current, 1 mA; magnetic field, 1.04 mT). In addition, atomic force microscopy (AFM) measurement was performed on the Au-coated ITO/glass substrate on a scan area of 5 × 5 μm^2. The sizes of Au particles were also estimated using AFM measurement.

RESULTS

The relationship between the Au thickness and the deposition time measured by AFM was constructed (Figure 3). The thickness linearly increased with the deposition time. Using the described coating condition, the deposition rate was approximately 2 $nm \cdot min^{-1}$. The particle size varied from 10 to 46 nm. It was expected that the Au films may be discontinuous up to a

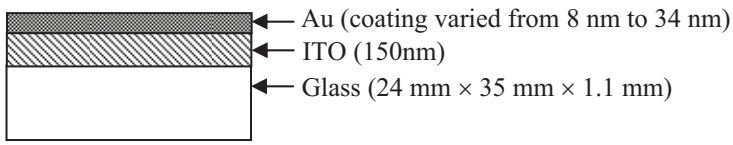

Figure 2 Schematic diagram of Au-coated indium tin oxide (ITO)/glass substrate.

Table 1 Sputtering conditions for Au thin films.

Sputtering condition				
Substrate	Sputtering pressure (mbar)	Current (mA)	Time (min)	Target diameter (mm)
1) ITO/glass 2) glass	9×10^{-2}	4	4-17	57

6 min coating time because a similar Au particle size was obtained on the substrate up to a 6-min coating time. In addition, the film's transparency and the fact that there was no electrical conduction on Au/glass films with the same coating condition suggested that discontinuous films were obtained and the electrical results are discussed in the following section.

Figure 4 shows the relationship between the sputtered Au thickness and the measured thin-film resistance of 1) Au/glass and 2) Au/ITO/glass. The resistance of Au/glass could be separated into three stages based on the Au thickness: stage I, below 10 nm; stage II, between 10 nm and 20 nm; and stage III, above 20 nm. In stage I, the resistance of Au/glass was relatively high compared to the other areas. In some cases, the resistance could not be measured because of the island-like structure. It was expected that once the first percolation path among the deposited clusters closed, the current began to flow. Then, the substantial decrease in the resistance was related to the increase in the number of paths becoming available for electron drifting as clusters interconnected (stage II). Earlier reports showed the morphology of the Au nanostructure on glass substrate where pin holes were still observed on the glass substrate even with an Au thickness at about 10 nm (Lansaker *et al.*, 2009), while Lansaker *et al.* (2009) showed that when the Au thickness ranged between 4.4 and 6.2 nm, the Au islands coalesced. There was no substantial difference in the sheet resistance of the Au/ITO/glass substrate and the resistance seemed to decrease monotonically as the Au thickness increased. This sugested that the contribution of the island-like Au films to the overall conductivity of the bi-layer system was similar to that of the continous Au thin films.

Figure 5 shows the relationship between the inverse resistance (1/R) and the estimated thickness of Au films on glass and ITO/glass substrates. In general, the relationship between the resistance is a linear function of 1/film thickness, so that when 1/R is plotted against thickness, a straight line should be observed as is clearly seen for the the Au/ITO/glass systems (Figure 5), while Au/glass did not show a similar linear behavior and these two datasets are not parallel. In particular, region 3 (above 20-nm Au thickness) can be considered as a continuous Au film. This indicated that the simple parellel circuit model between Au films and ITO films may not be suitable. Using the resistance of Au/glass, the conductivity of

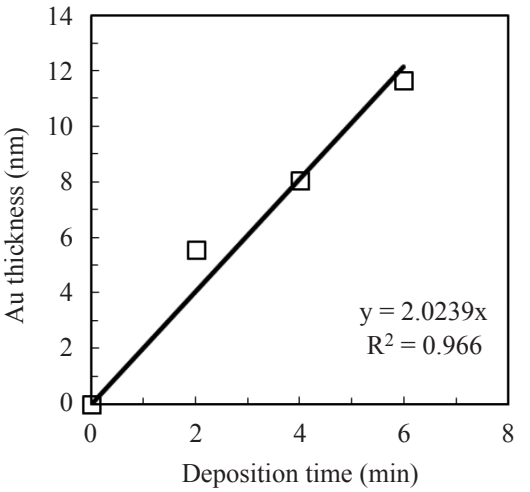

Figure 3 Relationship between Au thickness and deposition time (R^2 = Correlation coefficient; y = Au thickness; x = Deposition time).

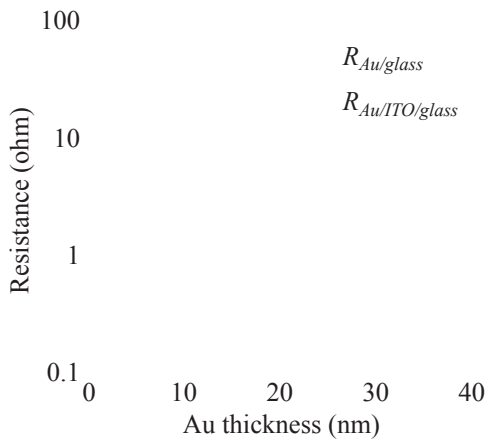

Figure 4 Relationship between resistance and estimated thickness of Au films on glass and Au films on indium tin oxide (ITO)/ glass substrates (I, II, III = Stages).

Au films can be calculated. The calculated Au conductivities ranging from 7.1×10^3 to 4.7×10^4 $\Omega^{-1}\cdot cm^{-1}$ are lower than the reported conductivity of metallic bulk Au of 4.3×10^5 $\Omega^{-1}\cdot cm^{-1}$ (Callister and Rethwisch, 2011). The lower conductivity of discontinous Au film was possibly due to the partial coverage of the films in the early coating stage.

DISCUSSION

As shown in Figure 4, three stages were apparent in the relationship between resistance and film thickness. In stage I, there were island-like Au nanoparticles, while in stage II, the Au nanoparticles became interconnected. In stage III, the two-dimensional Au film was completed. Barborini *et al.* (2010) also described conduction through the island-liked metallic films. The films evolved from 0D (islands) to 1D (sub-monolayer coverage) to 2D (thin films). The total resistance of the bi-layered thin film could be expressed using Equation 2:

$$\frac{1}{R_{total}} = \frac{1}{R_{Au}} + \frac{1}{R_{ITO}} \quad (2)$$

where R_{total} is the resistance of Au/ITO films on glass substrate and R_{Au} and R_{ITO} are the resistance of Au film and ITO film on glass, respectively.

However, this equation only holds when there is no effect due to the film boundary between Au and ITO. To verify this simple model, $1/R_{Au/ITO/glass}$ (or $1/R_{total}$) versus $1/R_{Au/glass}$ (or $1/R_{Au}$) was plotted as shown in Figure 6. Since, R_{ITO} is constant, Equation 2 would hold when the slope of the line equals 1 and the intercept on the $1/R_{Au/ITO/glass}$ axis is $1/R_{ITO}$. However, the obtained slope and the intercept were not as expected. Therefore, it is suggested that there should be other components to describe this behavior.

Two simple circuit models were developed to explain the observation. For the first model, the contact resistance (R_C) between the Au/ITO interface was introduced into the equation. The schematic diagram of the resistance model is shown in Figure 7a. In addition, the other simple model is shown in Figure 7b, where the imaginary interface resistance (R_I) was also added into the model, where R_I refers to the resistance created along the interface of Au/ITO.

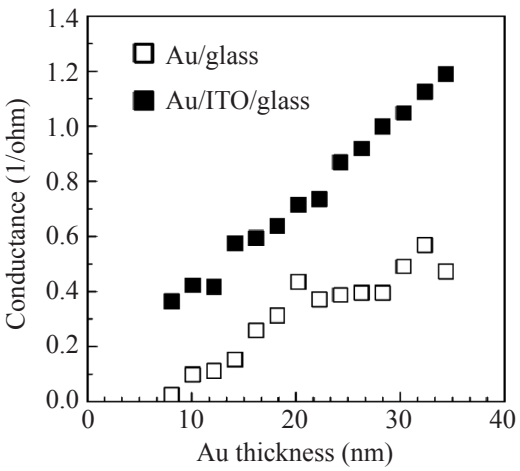

Figure 5 Relationship between inverted sheet resistance (conductance) and the estimated thickness of Au films on glass and indium tin oxide (ITO)/glass substrates.

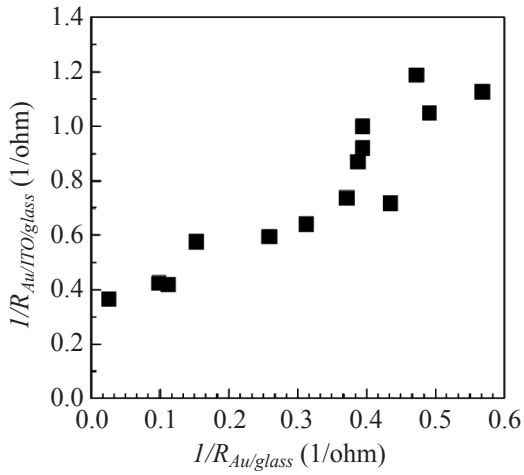

Figure 6 Relationship between the inverse of resistance of Au/indium tin oxide (ITO) films on glass substrate ($1/R_{Au/ITO/glass}$) and the inverse of resistance of Au film on glass ($1/R_{Au/glass}$).

When it is considered that R_{sp1} and R_{sp2} (the spreading resistances at the Au and ITO material, respectively) are much smaller than R_{Au} and R_{ITO}, the total resistance is shown by Equation 3:

$$\frac{1}{R_{total}} = \frac{1}{R_{Au}} + \frac{1}{R_{ITO} + 2R_C} \quad (3)$$

where R_{total} is the resistance of Au/ITO films on glass substrate and R_{Au} and R_{ITO} are the resistance of Au film and ITO film on glass, respectively and R_C is the contact resistance between Au and ITO.

Figure 7b shows the resistance model with interface resistance between Au and ITO thin films. Here, Equation 3 can be simplified to Equation 4:

$$\frac{1}{R_{total}} = \frac{1}{R_{Au}} + \frac{1}{R_{ITO}} + \frac{1}{R_I} \quad (4)$$

where R_{total} is the resistance of Au/ITO films on glass substrate, R_{Au} and R_{ITO} are the resistance of Au film and ITO film on glass, respectively, and R_I is the imaginary interface resistance.

Based on these two equations, a plot of R_C and R_I versus Au thickness is shown in Figure 8. The curves can be divided into two zones using the Au thickness of 20 nm as a separation point. Below 20 nm, the calculated R_I was negative while R_C was positive. Above 20 nm, the calculated R_I tended to increase and possibly became saturated, while the calculated R_C decreased and became negative. At an Au thickness below 20 nm, Au films were mostly discontinuous. It could be assumed that there was no contact resistance since the probe could penetrate through the Au films and contact the ITO films. Furthermore, the calculated R_C was also relatively small compared to the resistance of R_{ITO} and R_{Au} ; a positive R_C in this region may possibly have been due to the contribution of the island-like Au film. However, as the Au thickness increased, R_C became negative. Therefore, instead of using the contact-resistance model (Figure 7a), the observations suggested that there could be other factors causing the reduction in the bi-layered resistance at an Au thickness above 20 nm. As shown in Figure 8, R_I is small and positive at an Au thickness above 20 nm. The small and positive R_C in this range indicated that the decrease in resistance was possibly a result of the interface.

The Hall measurement was then conducted on three samples (150-nm ITO/glass, 4-nm Au/150-nm ITO/glass and 8-nm Au/150-nm ITO/glass). As shown in Table 2, the carrier concentrations of both bi-layered films were

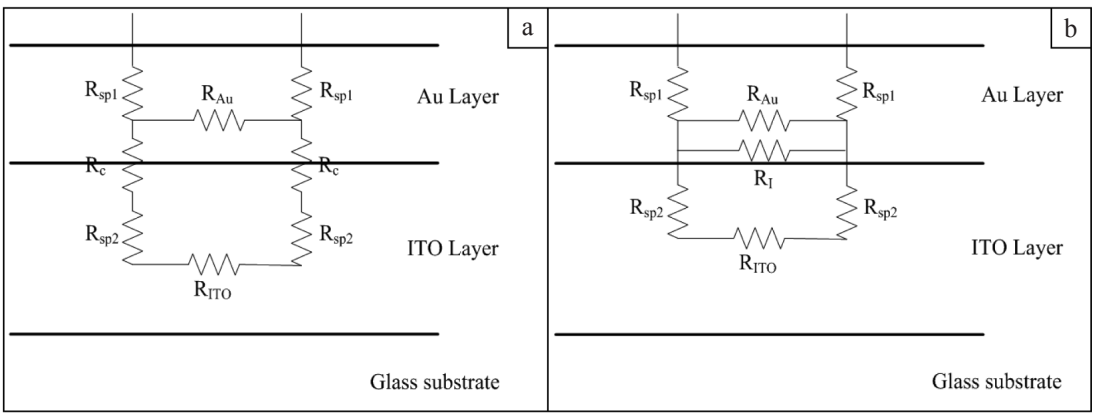

Figure 7 Schematic diagram of film resistance with: (a) Au/indium tin oxide (ITO) contact resistance; and (b) Au/ITO interface resistance. (R_C = Contact resistance between Au and ITO; R_I = Imaginary interface resistance; R_{sp1} and R_{sp2} = Spreading resistance at Au and ITO material, respectively.)

Table 2 Electrical properties of bare indium tin oxide (ITO) and Au-coated ITO.

Sample	Resistivity (Ω·cm)	Mobility ($cm^2 \cdot V^{-1} \cdot s^{-1}$)	Carrier concentration (cm^{-3})
150 nm ITO/glass	8.90×10^{-4}	12.3	5.69×10^{20}
4 nm Au/150 nm ITO/glass	1.61×10^{-4}	2.3	1.69×10^{22}
8 nm Au/150 ITO/glass	1.65×10^{-4}	4.6	8.22×10^{21}

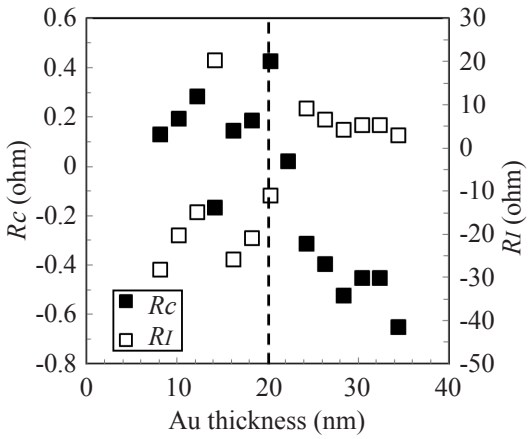

Figure 8 Relationships of contact resistance between Au and indium tin oxide (R_C) and imaginary interface resistance (R_I) versus Au thickness.

higher than for the bare ITO/glass substrate even when the 4-nm Au/glass and 8-nm Au/glass were expected to have an island-like structure. These results suggested that discontinuous Au films also contributed to the decrease in the resistivity. Kim (2010) observed similar results for the ITO/Au/ITO structure, reporting a reduction of mobility as the Au thickness increased and it was suggested that the Au/ITO interface could be the source of the increase in carrier concentration. Furthermore, as the surface states increased, the mobility decreased. The observation of saturated R_I (Figure 8) could have been the result of the completion of the interfaces. No extra carriers were generated when the Au films become continuous.

CONCLUSION

A simple model was developed to identify the electrical characteristics of low-coverage Au on an ITO/glass substrate. The Au islands contributed to the conduction of this bi-layered film. The possibility of increased conductivity in the bi-layered thin film was a result of the interface causing an increase in the carrier concentration and a reduction of mobility. Further investigation to confirm the phenomena is needed.

ACKNOWLEDGEMENTS

The authors would like to acknowledge financial support from the Faculty of Science, King Mongkut's University of Technology Thonburi and to thank Mr. Thanyathep Nantachai and Mr. Thanawat Summalertphant for their diligent work with the four-point probe measurements.

LITERATURE CITED

Aiempanakit.K., P. Rakkwamsuk and S. Dumrongrattana. 2008. Characterization of indium tin oxide films after annealing in vacuum. **Kasetsart J. (Nat. Sci.)** 42: 351–356.

Barborini, E., G. Corbelli, G. Bertolini, P. Repetto, M. Leccardi, S. Vinati and P. Milani. 2010. The influence of nanoscale morphology on the resistivity of cluster-assembled nanostructured metallic thin films. **New J. Phys.** 12: 073001(1)–073001(12).

Bender, M., W. Seelig, C. Daube, H. Frankenberger, B. Ocker and J. Stollenwerk. 1998. Dependence of film composition and thicknesses on optical and electrical properties of ITO-metal-ITO multilayers. **Thin Solid Films** 326: 67–71.

Callister, W.D. and D.G. Rethwisch. 2011. **Fundamentals of Materials Science and Engineering: An Integrated Approach.** 4th ed. Wiley-Interscience. Hoboken, NJ, USA. 910 pp.

Choi, J.I., J.Y. Lee, J.H. Park, J.H. Chae, H.J. Park, D. Kim. 2009. Fabrication and characterization of Pt intermediate transparent and conducting ITO/Pt/ITO multilayer films. **J. Phys. Chem. Solids.** 70(2): 272–275.

Feng T. and A.K. Ghosh (inventors); Exxon Research & Engineering Co. (assignee). 1979. Method of fabricating conducting oxide-silicon solar cells utilizing electron beam sublimation and deposition of the oxide. **US Patent 4,177,093.** 4 December 1979.

Ke, L., R. Senthil, P. Chen, L. Shen, S. Chua and A.P. Burden. 2005. Au-ITO anode for efficient polymer light-emitting device operation. **IEEE Photonics Tech. L.** 17: 543–545.

Kim, D. 2010 Low temperature deposition of transparent conducting ITO/Au/ITO films by reactive magnetron sputtering. **Appl. Surf. Sci.** 256: 1774–1777.

Klinghult G. and P. Futter (inventors); Klinghult G. and P. Futter (assignees). 2009. Pen stylus enabled capacitive touch system and method. **US Patent US20090256825 A1.** 15 October 2009.

Lansaker, P.C., J. Backholm, G.A. Niklasson and C.G. Granqvist. 2009. TiO_2/Au/TiO_2 multilayer thin films: novel metal-based transparent conductors for electrochromic devices. **Thin Solid Films.** 518: 1225–1229.

Nakamura, M., H. Ohguri, H. Yanagisawa, N. Goto, N. Ohashi and K. Kudo. 2003. Electrical characterization of pentacene thin films using four-point-probe field-effect measurement and atomic force microscope potentiometry, pp.130–135. *In* **Proc. Int. Symp. Super-Functionality Organic Devices. IPAP Conf.** 25–28 October 2004. Chiba, Japan.

Novoselov, K.S., A.K. Geim, S.V. Morozov, D. Jiang, Y. Zhang, S.V. Dubonos, I.V. Grigorieva and A.A. Firsov. 2004. Electric field effect in atomically thin carbon films. **Science** 306: 666–669.

Pokaipisit, A., M. Horprathum and P. Limsuwan. 2007. Effect of films thickness on the properties of ITO thin films prepared by electron beam evaporation. **Kasetsart J. (Nat. Sci.)** 41: 255–261.

Schroder, D.K. 2006. **Semiconductor Material and Device Characterization.** 3rd ed. Wiley-Interscience. Hoboken, NJ, USA. 779 pp.

Vu, Q. T., E. Kolawa, L. Halperin and M.-A. Nicolet. 1991. Specific contact resistance extraction from four-point-probe measurements on multilayered film structures. **Solid-State Electron.** 34: 279–283.